Biomaterials 33 (2012) 8277–8285

Contents lists available at SciVerse ScienceDirect

Biomaterials

journal homepage: www.elsevier.com/locate/biomaterials

Functionality, growth and accelerated aging of tissue engineered living autologous vascular grafts

Jens M. Kelm [a,b,1], Maximilian Y. Emmert [a,c,1], Armin Zürcher [b], Dörthe Schmidt [a], Yvonne Begus Nahrmann [d], Karl L. Rudolph [d], Benedikt Weber [a], Chad E. Brokopp [a], Thomas Frauenfelder [e], Sebastian Leschka [e], Bernhard Odermatt [f], Rolf Jenni [g], Volkmar Falk [c], Gregor Zünd [a], Simon P. Hoerstrup [a,b,c,*]

[a] Swiss Centre for Regenerative Medicine, University Hospital and University of Zurich, Zurich, Switzerland
[b] Competence Center for Applied Biotechnology and Molecular Medicine, Microscale Tissue Engineering Group, VetSuisse Faculty, University of Zurich, Zurich, Switzerland
[c] Clinic for Cardiovascular Surgery, University Hospital Zurich, Zurich, Switzerland
[d] Institute of Molecular Medicine and Max-Planck-Research Group on Stem Cell Aging, University of Ulm, Ulm, Germany
[e] Department of Radiology, University Hospital Zurich, Zurich, Switzerland
[f] Department of Pathology, University Hospital Zurich, Switzerland
[g] Clinic for Cardiology, University Hospital Zurich, Zurich, Switzerland

ARTICLE INFO

Article history:
Received 11 April 2012
Accepted 24 July 2012
Available online 18 August 2012

Keywords:
Tissue engineering
Tissue engineered vascular grafts
Aging
Telomere length
Growth
Pulmonary artery

ABSTRACT

Living autologous tissue engineered vascular-grafts (TEVGs) with growth-capacity may overcome the limitations of contemporary artificial-prostheses. However, the multi-step *in vitro* production of TEVGs requires extensive *ex vivo* cell-manipulations with unknown effects on functionality and quality of TEVGs due to an accelerated biological age of the cells. Here, the impact of biological cell-age and tissue-remodeling capacity of TEVGs in relation to their clinical long-term functionality are investigated. TEVGs were implanted as pulmonary-artery (PA) replacements in juvenile sheep and followed for up to 240 weeks (~4.5years). Telomere length and telomerase activity were compared amongst TEVGs and adjacent native tissue. Telomerase-activity of *in vitro* expanded autologous vascular-cells prior to seeding was <5% as compared to a leukemic cell line, indicating biological-aging associated with decreasing telomere-length with each cellular-doubling. Up to 100 weeks, the cells in the TEVGs had consistently shorter telomeres compared to the native counterpart, whereas no significant differences were detectable at 240 weeks. Computed tomography (CT) analysis demonstrated physiological wall-pressures, shear-stresses, and flow-pattern comparable to the native PA. There were no signs of degeneration detectable and continuous native-analogous growth was confirmed by vessel-volumetry. TEVGs exhibit a higher biological age compared to their native counterparts. However, despite of this tissue engineering technology related accelerated biological-aging, growth-capacity and long-term functionality was not compromised. To the contrary, extensive in-vivo remodeling processes with substantial endogenous cellular turnover appears to result in "TEVG rejuvenation" and excellent clinical performance. As these large-animal results can be extrapolated to approximately 20 human years, this study suggests long-term clinical-safety of cardiovascular *in vitro* tissue engineering and may contribute to safety-criteria as to first-in-man clinical-trials.

1. Introduction

Congenital cardiovascular malformations are a major cause of morbidity and mortality and occur in 1% of live births [1]. These malformations including abnormalities of the left and right ventricular outflow tract and great arteries often require complex and reconstructive surgical interventions and the use of artificial vascular graft prostheses. However, a critical limitation of the currently available artificial (non-living) graft prostheses is their inherent lack of growth [2] often requiring repetitive and high-risk surgical interventions during childhood associated with substantially increased morbidity and mortality. These shortcomings have been addressed by evolving tissue engineering concepts, focusing on the *in vitro* creation of living autologous tissue engineered

* Corresponding author. Swiss Centre for Regenerative Medicine and Clinic for Cardiovascular Surgery, University Hospital and University of Zürich, Raemistrasse 100, CH 8091 Zurich, Switzerland. Tel.: +41 44 255 3801; fax: +41 44 255 4369.
E-mail address: simon_philipp.hoerstrup@usz.ch (S.P. Hoerstrup).
[1] These authors contributed equally to the manuscript.

0142-9612/$ – see front matter © 2012 Elsevier Ltd. All rights reserved.
http://dx.doi.org/10.1016/j.biomaterials.2012.07.049

replacements with the capacity of growth and regeneration [3–6]. Previously, we have demonstrated that *in vitro* tissue engineered vascular-grafts (TEVGs) based on autologous cells exhibit functionality and growth in a growing sheep-model, approximating their native counterparts as to morphology, microstructure, cellular profiles and mechanical properties [3].

However, the multi-step *in vitro* production of TEVGs requires extensive *ex vivo* cell manipulations including cell isolation, primary cell culture, cell expansion, cell seeding on the vascular graft and maturation in a bioreactor system [7,8] potentially leading to adverse effects that may compromise clinical safety. In particular, accelerated cell aging has been associated with tissue engineering concepts. Variations in telomere length have been shown to affect tissue function due to senescence if telomeres become too short [9–19]. This might compromise clinical safety through accelerated aging phenomena with potential adverse effects on the long-term *in vivo* functionality of the TEVGs [10–12,16–19] as cells are extensively expanded prior graft production. In the present study, we investigated the clinical long-term functionality in relation to the biological cell age and tissue remodeling of TEVGs in a growing sheep model over the period of up to 240 weeks (~4.5 years), representing the complete growth cycle of this preclinical large animal model.

2. Materials and methods

The analysis performed here and the results presented in this study are partly based on tissue samples generated in a previous study focusing on functional growth of tissue engineered arteries in long-term juvenile sheep model [3].

2.1. In vitro production and implantation of tissue engineered vascular grafts

Production and implantation of pulmonary artery replacements is described in detail previously [3]. All procedures were conducted according to Swiss regulations on animal welfare and permission granted by the ethical committee (Permission No. 71/2002, 91/2004). Briefly, endothelial cells were obtained from segments of carotid artery, saphenous vein and/or jugular vein derived from Swiss White Alpine lambs (44 ± 2 days old, 15.58 ± 5.55 kg; $n = 6$) using collagenase digestion. Myofibroblasts were extracted from the remaining de-endothelialized vessel segments [3]. Thereafter, myofibroblasts were seeded in three times onto PGA/P4HB composed arterial scaffolds (18 mm ± 1 mm, inner diameter) in 24 h intervals ($4.5–5.5 \times 10^6$ cells per cm^2) under static culture conditions using Dulbecco's modified Eagle's medium (DMEM, Invitrogen, Carlsbad, CA) supplemented with 10% lamb serum (GibcoBRL; Cat. No. 16070096 Lot. No. 6050576D), Penicillin/Streptomycin (GibcoBRL) and 10 mM ascorbic acid. Thereafter, the conduits were covered with endothelial cells (1×10^6 per cm^2). After additional 3 days grown under static culture conditions, the vascular grafts were placed into a pulse duplicator bioreactor system [6], and grown under gradually increasing flow conditions (50 mL/min–550 mL/min, 1 Hz) for 14 days. The culture medium was changed every 3–4 days.

The tissue engineered vascular grafts were implanted into lambs ($n = 14$) as previously described [3]. Experimental duration was up to 240 weeks, representing the full biological growth cycle of this animal model. Animals included in this study were analyzed after 5, 50, 100 and 240 weeks post mortem.

2.2. "Re-growing" of myofibroblasts

Tissue sections (23×5 mm in size) of explanted TEVGs and adjoining tissues were obtained. Specimens were rinsed with PBS (Kantonsapotheke, Zurich, Switzerland) and placed in cell culture dishes (Nunc, Denmark). In order to obtain myofibroblasts, endothelial cells were removed using collagenase as described before [3]. The remaining de-endothelialized vessel segments were minced into pieces ($3 \text{ mm} \times 3 \text{ mm}$) and placed in cell culture dishes and cultured in advanced DMEM (GIBCO, NY, USA) supplemented with 10% lamb serum, 2 mM Glutamax (GIBCO, NY USA) and 50 μg/ml gentamycin (GIBCO, NY USA.) under humidified incubator conditions (37 °C, 5% CO_2). After myofibroblast migration onto the dishes (5–7 days), the cells were serially passaged and expanded. After 14–16.5 doublings, cells were harvested using trypsin digestion (GIBCO, NY USA.) and cell phenotypes by FACS, telomere length as well as cell morphology were analyzed.

2.3. Flowcytometry (FACS)

For quantification of antigen expression of TEVG-derived cells and their native counterparts FACS-analysis was performed using antibodies against vimentin (clone 3B4), desmin (clone D33), α-smooth muscle actin (α-SMA, clone 1A4; all from DakoCytomation, Glostrup, Denmark). Therefore, cells were fixed and permeabilized using an inside stain kit (Miltenyi, Biotech, Bergisch Gladbach, Germany) following the manufacturer's instructions. Primary antibodies were detected with fluorescein isothiocyanate (FITC)-conjugated goat anti-mouse antibodies (Boehringer Mannheim, Indianapolis, IN). Analysis was performed on a Becton Dickinson FACScan (Sunnyvale, CA). Irrelevant isotype-matched antibodies (IgG1MOPC-21, Buchs, Switzerland; IgG2a, cloneUPC-10, Sigma, Switzerland) served as negative controls and human vascular-derived fibroblasts as positive controls. Geometric mean fluorescence intensity ratios (MFIR) were calculated as:

$$\frac{\text{MFI}_{\text{ABI}}}{\text{MFI}_{\text{ABC}}} \tag{1}$$

ABI: Antibody of interest; ABC: Corresponding control antibody, MFI, Mean fluorescent intensity.

2.4. Histo and immunohistological analysis

Immunohistochemistry was performed using the Ventana Benchmark automated staining system (Ventana Medical Systems, Tuczon, Arizona) and following primary antibodies: anti-desmin (clone D33, DakoCytomation, Glostrup, Denmark) and anti-α-smooth muscle actin (α-SMA, clone 1A4; Sigma Chemical Company, St. Louis, MO). Primary antibodies were detected with the Ventana iVIEW DAB detection kit, resulting in a brown reaction product. Slides were counterstained with hematoxylin and covered with a glass cover slip.

2.5. Flow FISH

To determine the relative telomere length (RTL) of expanded myofibroblasts flow fish analysis was performed according to manufacturer's protocol (DakoCytomation). Briefly, myofibroblasts were harvested from cell culture flasks using standard cell culture protocols. The single cell solutions were washed twice with phosphate buffered saline and the hybridization solution (DakoCytomation) containing the FITC-labeled PNA probe, targeted to the repetitive telomere sequence TTAGGG, added. Afterward the DNA was denatured for 15 min at 82 °C and hybridized over night at room temperature. Following hybridization the cells were washed twice with wash solution (DakoCytomation) for 10 min at 40 °C and resuspended in DNA-staining solution containing propidium iodide (PI) and RNase A. After incubation of at least 2 h at 4 °C samples were measured using a fluorescent cell sorter (Beckman Coulter, Cytomics FC500, Fullerton, CA) and analyzed with CXP software (Beckman Coulter). PI was used to detect cells in G0/G1 cell cycle state. As control cell line tetraploid human lymphoblastic T cell line 1301 (obtained from Interlab Cell Line Collection (IST), Genova, Italy) was used. Relative telomere length (RTL) was calculated as:

$$\frac{(\text{MFI}_{\text{MF With PNA}} - \text{MFI}_{\text{MF without PNA}})^{*}2_{\text{DNAIndex1301}}}{\text{MFI}_{1301\text{ With PNA}} - \text{MFI}_{1301\text{ without PNA}}} * 100 = \text{RTL} \tag{2}$$

MFI: mean fluorescent intensity; MF: sheep myofibrolasts; PNA: FITC-labeled telomere PNA probe; RTL: relative telomere length; 1301: leukemic human control cell line with high telomerase activity.

2.6. Telomeric Repeat Amplification Protocol (TRAP)

Telomerase activity was measured using the telomeric repeat amplification protocol (TRAP) according to the kit's manufacturer (Telo*TAGGG* Telomerase PCR ELISA, Roche Diagnostics GmbH, Switzerland). Cell pellets consisting of 2x10E5 cells were stored at −80 °C. The samples were resuspended in Lysis reagent (Roche-Diagnostics) and incubated on ice for 30 min. Afterward, the lysate was centrifuged at 4 °C and 16000 × g for 20 min before performing the TRAP reaction. For negative controls, cell extracts were heat treated for 10 min at 85 °C prior to the TRAP reaction. 3 ul of the cell extract were used for the reaction. As positive controls cell lysates provided by the supplier as well as from the leukemic cell line 1301 were used. The reaction mixture (Roche Diagnostics) containing Telomerase substrate, primers, nucleotides and Taq polymerase were transferred to Eppendorf tubes suitable for PCR amplification. The amplification was performed using an Eppendorf Mastercycler (Eppendorf, Netheler, Germany). The elongation of a biotin-labeled synthetic primer by the telomerase enzyme leads to non-uniform "elongation products" (telomerase specific 6 nucleotide increments). These were then amplified by Taq DNA Polymerase. The amplification product was denatured and incubated for 10 min at room temperature (Denaturation reagent, Roche Diagnostics), then hybridized over 2 h at 37 °C (Hybridization buffer, Roche Diagnostics) to digoxigenin-labeled detection probes. The hybridization mixtures were transferred to streptavidin-coated microplate modules and incubated for an additional hour at 37 °C. The wells were washed (washing solution, Roche Diagnostics) three times before Anti-DIG-POD working solution (containing anti-digoxigenin-peroxidase, Roche Diagnostics) was added. The plate was covered with foil and incubated for 30 min at room temperature while shaking at 300 rpm. The samples were rinsed 5 times (washing solution, Roche diagnostics) and TMB substrate solution (Roche diagnostics) containing the POD substrate 3,3′,5,5′-tetramethyl benzidine was

added. After 20 min of color development at room temperature, the stop reagent (Roche diagnostics) was added and the absorbance at 450 nm was measured against blank of 750 nm using a microplate reader (BioTek Instruments, Inc, VT, US) within 20 min after addition of the stop reagent.

2.7. Quantitative fluorescent in-situ hybridisation (Q-FISH)

Paraffin sections of cryopreserved tissue engineered explanted grafts, the anastomosis site and its adjacent vascular tissue, respectively, were dewaxed and rehydrated in descending ethanol series and rinsed with PBS. After incubation in sub-boiling citrate buffer for a cumulative 30 min, the slides were incubated for 10 min in pepsin solution (1 mg/ml,pH 2.0) at 37 °C. After dehydration in ascending ethanol series, the slides were air dried before adding 15 ul of the hybridization mix containing 70% formamide, 0.5 ug/ml PNA probe (5 ul/250 ul, 25 ug/ml PNA), 0.5% Blocking reagent (12.5 ul/250 ul, 10% Solution, Roche), 8.56% Magnesiumchloride buffer (25 mM Magnesiumchloride, 9 mM Citric acid, 82 mM Disodium hydrogenphosphate) and 10% 1 M Tris pH 7.2. DNA was denatured by heat for 3 min at 80 °C. After hybridization for 2 h in a humid chamber, slides were washed with 70% formamid/10 mM Tris pH 7.2/0.1% BSA followed by TBS-Tween 1% and PBS. Slides were dehydrated using ascending ethanol series and air dried. Antifade and DAPI (Vectashield, Vector #H1200) mounting solution and a cover slip was applied. Digital images were recorded with a Leica microscope (DM6000, Leica Microsystems, Wetzlar, Germany) equipped with a monochromatic digital camera (Leica Microsystems). Image analysis was performed with TFL-Telo software as describe by Poon and Landsorp [20].

2.8. Computed tomography analysis

All sheep underwent contrast enhanced Computed Tomography (CT) (Definition, Siemens Medical Solutions, Forchheim, Germany). Based on these datasets two different types of analyses were performed: (1) Simulation of flow inside the pulmonary artery to evaluate the changes in wall shear stress and pressure (2) Measurement of the volume of pulmonary artery replacement to validate the functional growth.

2.9. Flow simulation

Axial CT images were digitally processed to extract geometrical contours representing the pulmonary trunk and main plumonary arteries, including the pulmonary artery replacement.

The lumen of these vessels was semi-automatically segmented using a commercially available software package (Amira 4.1, TGS, Belgium). As a next step, an unstructured surface mesh of triangles was generated covering the segmented volume using the marching cube algorithm [21,22]. Manual smoothing and low-pass spatial filtering was then applied to further reduce fine-scale surface irregularities. The final model depicted the real 3D geometry of the pulmonary vessels (Suppl Fig. 1).

Geometric computational models were subsequently built with computational meshes of 800,000–1,000,000 tetrahedral cells for the entire models. This model was used for pulsatile blood flow simulations for the entire cardiac cycle. The following model assumptions and boundary conditions were made. The flow for the simulation was considered transient, 3D, incompressible, and laminar (based on the low Reynolds number of approximately 300 for small vessels). Corresponding to standard values from the literature [23] the blood was assumed to be Newtonian with a viscosity of 0.0037 Pa s and a density of 1060 kg/m^3. The walls were taken as solid and stiff, and a zero-velocity boundary condition was assumed for the walls, corresponding to a no-slip condition. The flow velocity profile at the different inlets was based on standard data reflecting the physiologically pulsatile, biphasic blood flow from the pulmonary artery. The FLUENT software (Ansys Corp., Darmstadt, Germany) was used to carry out the simulation by solving Navier–Stokes equations. The calculated flow variables were flow velocities, WSS, and wall pressure. The CFD Post software (Ansys Corp., Darmstadt, Germany) was used for the visualization of flow patterns, the quantification of wall shear stress and wall pressure.

2.10. Vessel volumetry

The volume of the pulmonary artery replacement was measured applying a dedicated software (3surgery, 3mensio, Bilthoven, the Netherlands). To standardize the measurement a defined length of 2 cm of the TEVG (based on CT imaging) was included.

2.11. Statistical analysis

Statistical analysis including histograms and boxplots was carried out with PASW statistics version 18 for windows (SPSS Inc., Chicago, IL, USA). Q-FISH data underwent the Mann-Whitney-U-test for statistical significance. The null-hypothesis was rejected for p-values greater than 0.05.

3. Results

3.1. Telomere shortening and tissue remodeling

To gain sufficient cell numbers for the production of TEVG cells have to be expanded *in vitro* extensively, up to 3×10^8 cells are required for one construct. To assess biological aging during the expansion phase, myofibroblasts derived from the saphenous and jugular veins were evaluated with respect to their telomerase activity and capacity to maintain telomeres during cell expansion. Telomerase-activity of cultured myofibroblasts was less than 5% compared to positive controls (lysates provided by the kit supplier and lysates from 1301 leukemic cells) (Fig. 1A). Although native telomere-length is genetically determined and varies between individuals [24], decrease of the telomere-length during cell expansion *in vitro* was in direct correlation with increasing population doublings (Fig. 1B).

To compare the biological age of the TEVGs and the native pulmonary artery, longitudinal sections harboring both specimen enabled a direct side by side comparison of the telomere-length by quantitative in-situ (Fig. 2). Up to 10 areas of both specimens were

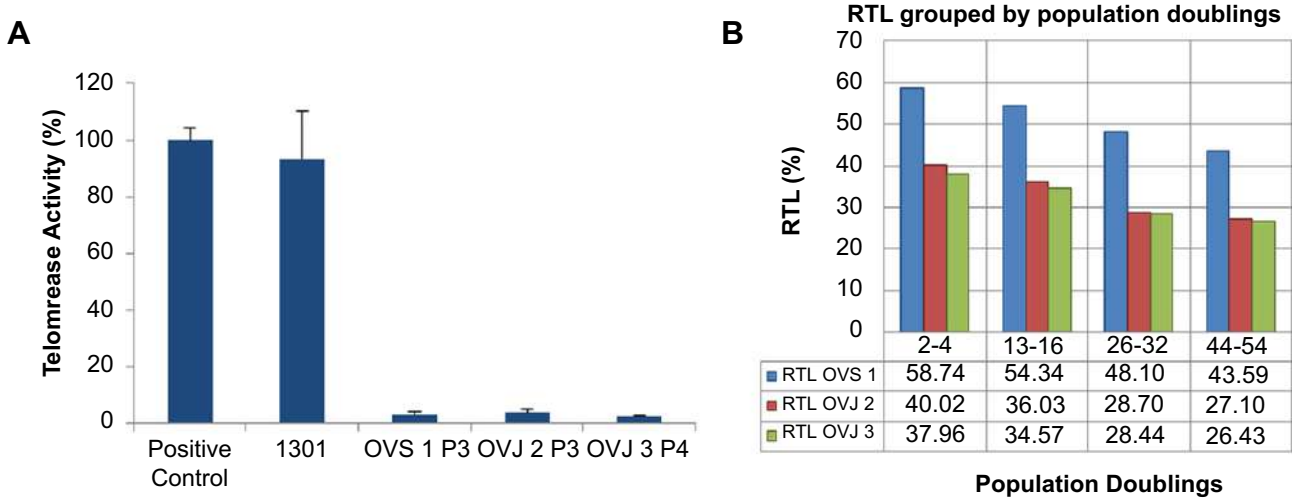

Fig. 1. (A) Telomerase activity of ovine myofibroblasts isolated from saphenous vein (VS) and jugular vein (VJ) of 3 individual lambs (OVS1, OVJ2 and OVJ3). Telomerase activity was absent in all three cell isolates as compared to the control lymphocyte cell line 1301. (B) Even if there are differences in the initial relative telomere length (RTL), its decrease with incremental population doublings during *in vitro* cell expansion which is comparable for all cell isolations.

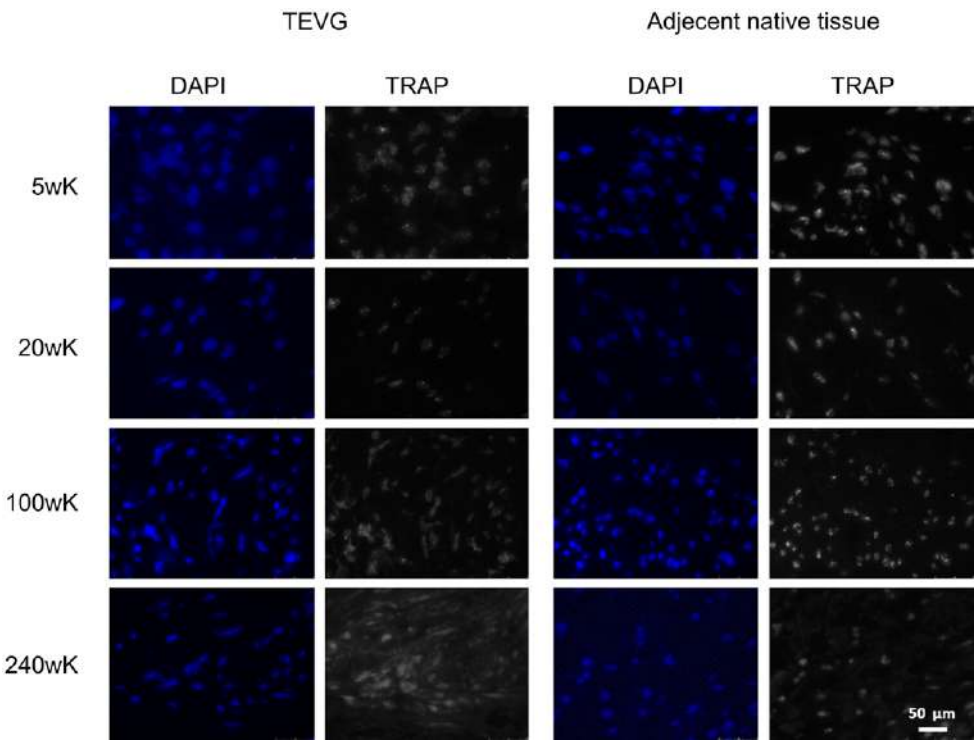

Fig. 2. Exemplified images taken from the TEGVs and adjacent native pulmonary artery used for the TRAP analysis. Comparison was performed always on the same section. Nuclei are shown in blue (DAPI) and telomeres in white (TRAP) (For interpretation of the references to colour in this figure legend, the reader is referred to the web version of this article.).

imaged and the fluorescence intensity quantified. Over a total period of 240 weeks (~4.5 years), it was demonstrated that up to 100 weeks, the cells in the TEVGs have consistently shorter telomeres compared to cells in the corresponding native artery. The Mann-Whitney-U-Test confirmed statistical differences for the distribution with a *p*-value below 0.01 for the samples derived after 5, 20 and 100 weeks. However, after 240 weeks no significant differences were detectable anymore (Table 1). The relative telomere length in the specimen displayed no shift of the TEVG cell populations toward the native cell population. Up to 100 weeks after implantation the cells within the TEVGs displayed an approximately 60% lower relative telomere length than their native counterparts (Table 1). After 240 weeks there is no significant difference observed, however the signal intensity in the native PA displayed a lower value as at the earlier explant time points (Table 1). To confirm that similar cell population were investigated myofibroblasts from the TEVGs and native pulmonary artery were isolated and regrown for FACS analysis. The cellular phenotypes of both cell populations displayed comparable expression levels of vimentin and α-SMA and the lack of Desmin indicating similar cell composition in both populations (Fig. 3).

Table 1
Quantification of measured fluorescence intensity obtained by the telomeric repeat amplification protocol (TRAP) from specimens 5, 20, 100 and 240 week explants. Telomere length of cells of the tissue engineered and native areas was performed always on the same section. The Mann-Whitney-U-Test confirmed statistical differences for the distribution with a *p*-value below 0.01 for the samples derived after 5, 20 and 100 weeks. However, after 240 weeks, no significant difference could be detected.

	TEVG	Native		TEVG	Native
5 weeks			20 weeks		
Mean	1386	2149	Mean	1595	2996
Median	1004	1211	Median	954	1622
Std. deviation	1122	2502	Std. deviation	1727	3400
100 weeks			240 weeks		
Mean	1245	1967	Mean	1012	1033
Median	856	1114	Median	664	660
Std. deviation	1255	2376	Std. deviation	1038	1116

In addition to the accelerated cell aging during the expansion-phase *in vitro*, substantial *in vivo* remodeling processes of the TEVGs associated with increased DNA and extracellular matrix contents were detected [3]. Histological specimens from the sites of anastomosis suggest that the tissue engineered construct is increasingly populated with native cells as displayed by the formation of a "growth cone" with elevated levels of Desmin and α-SMA positive cells 20 weeks after implantation (Fig. 4A and B). Whereas the interface between the TEVG and the native PA is still detectable after 20 weeks it is less prominent after a 100 weeks (Fig. 4C and D) and hardly visible after 240 weeks *in vivo* (Fig. 4G–J), indicating completion of tissue remodeling beyond 100 weeks. The histological evaluation of the side of anastomosis suggests that the TEVGs are repopulated from the native PA. Biochemical analysis revealed slightly lower DNA content, similar amount of proteoglycans and increased collagen contents in all TEVGs, when compared to the native vessel (Suppl Fig. 2) indicating either recruitment of endogenous cells or further maturation and proliferation of the cell population used to produce the TEVGs.

3.2. Evaluation of long-term functionality and growth of TEVGs

In the initial study basic functionality as well as growth over the complete biological growth cycle of this animal model was demonstrated using trans-esophageal echocardiography (TEE) and computed tomography [3]. Based on the computed tomography raw data of the initial study [3], two different types of analyses were performed to confirm long-term functionality and growth: (1) Simulation of flow inside the pulmonary artery to evaluate the changes in wall shear stress and pressure (2) Measurement of the

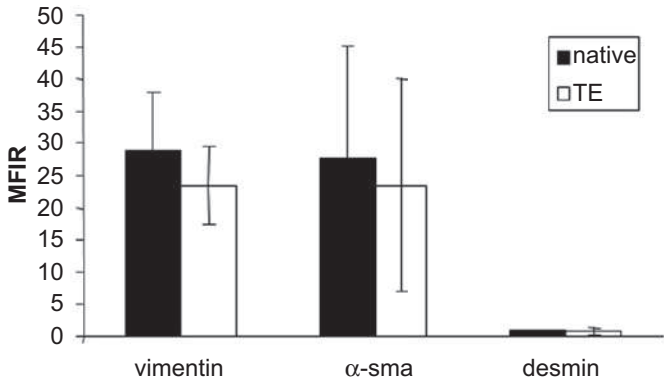

Fig. 3. Expression of vimentin, a-SMA and desmin in ovine tissue engineered construct-derived myofibroblast after 100 weeks *in vivo* compared to their native counterparts analyzed by flowcytometry. Expressions are shown as MFIR (mean fluorescence intensity radio divided by mean fluorescence intensity of corresponding isotype control) ± standard deviations.

volume of pulmonary artery replacement to validate the functional growth. The 3D CT reconstruction and flow simulation analysis demonstrated a sufficient and stable wall pressure (Fig. 5A and B, Suppl Trailer 1), shear stress (Fig. 5A and B, Suppl Trailer 2), and flow velocity (Fig. 5C and D, Fig. 6I, Suppl Trailer 3), in the pulmonary-trunk during systoly and diastoly for up to 240 weeks. In detail, the CT displayed a smooth flow pattern (Fig. 5C and D, Fig. 6I, Suppl Trailer 3) and low wall pressure during systoly at all time points, up to 240 weeks (Fig. 5A and B, Suppl Trailer 1). The low wall shear stress (Fig. 5A and B, Suppl Trailer 2) and the absence of turbulences confirmed native analogous vascular performance and absence of degenerative phenomena, such as atherosclerotic calcifications, thrombus formation, stenosis, suture dehiscence, or aneurysm formation which was confirmed macroscopically at the time point of harvest (240 weeks after implantation) (Fig. 6J–K). In addition, continuous functional growth was demonstrated by CT volumetry measurements, displaying a significant volume increase of the TEVGs from an initial volume of 6.4 ccm 20 weeks after implantation (Fig. 6C) up to 13.2 ccm after 240 weeks (Fig. 6F) corresponding to the increase of body weight of the animals.

Supplementary data related to this article can be found online at http://dx.doi.org/10.1016/j.biomaterials.2012.07.049.

In addition to the trans-esophageal echocardiography (TEE) analysis displaying no signs of malfunction or degeneration such as thrombus formation, calcification, stenosis, suture dehiscence, or aneurysm formation at 100 weeks post implantation [3], these findings could be also confirmed on TEE at the 240 weeks follow up demonstrating an excellent long-term functionality (Fig. 6G and H).

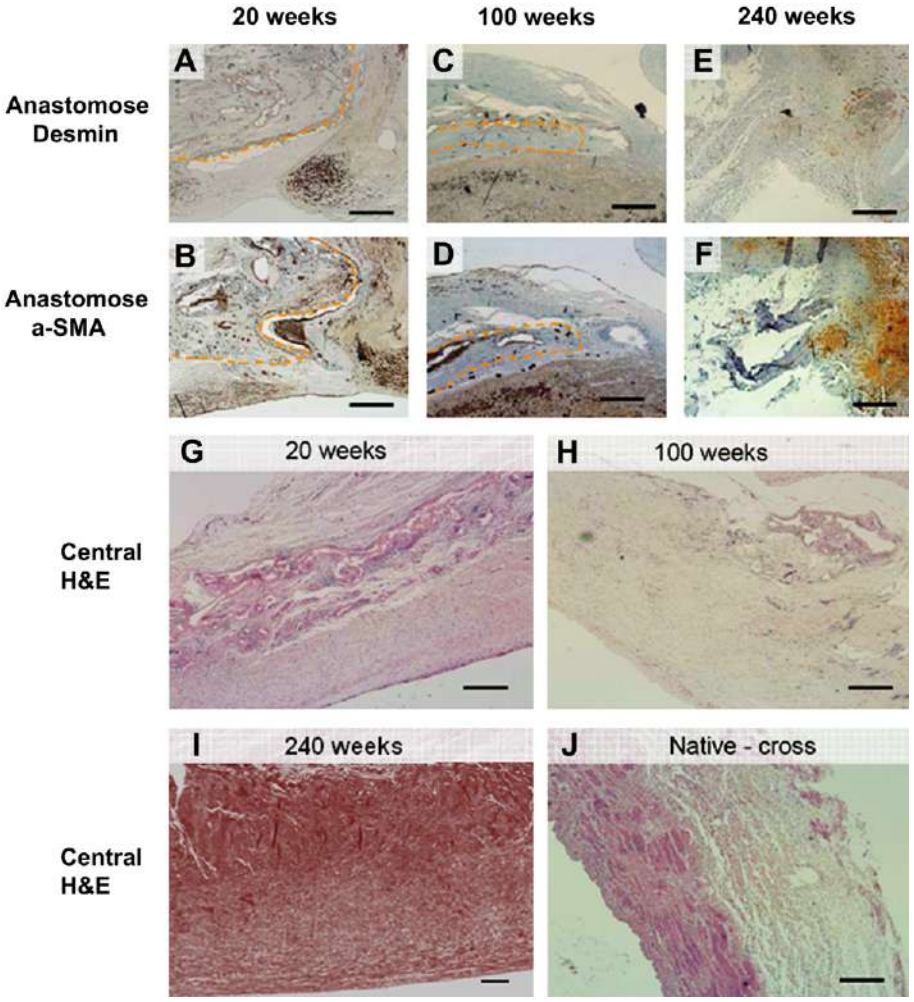

Fig. 4. Histological analysis of the remodeling process of tissue engineered vascular grafts 20 (A, B, G), 100 weeks (C, D, H) and 240 weeks (E, F, I) After implantation into lambs as well as an H&E staining from a native pulmonary artery (J). A kind of growth cone formation was observed 20 weeks after implantation enclosing the tissue engineered graft (indicated with the dotted line) composed of cells positive for desmin (A) and α-SMA (B) at the sides of anatomizes. These growth were not observed 100 weeks post-implantation (C, D). The remodeling process within the inner core of the transplant is shown in with an H&E staining in G, H and I. Scalebar = 500 μm.

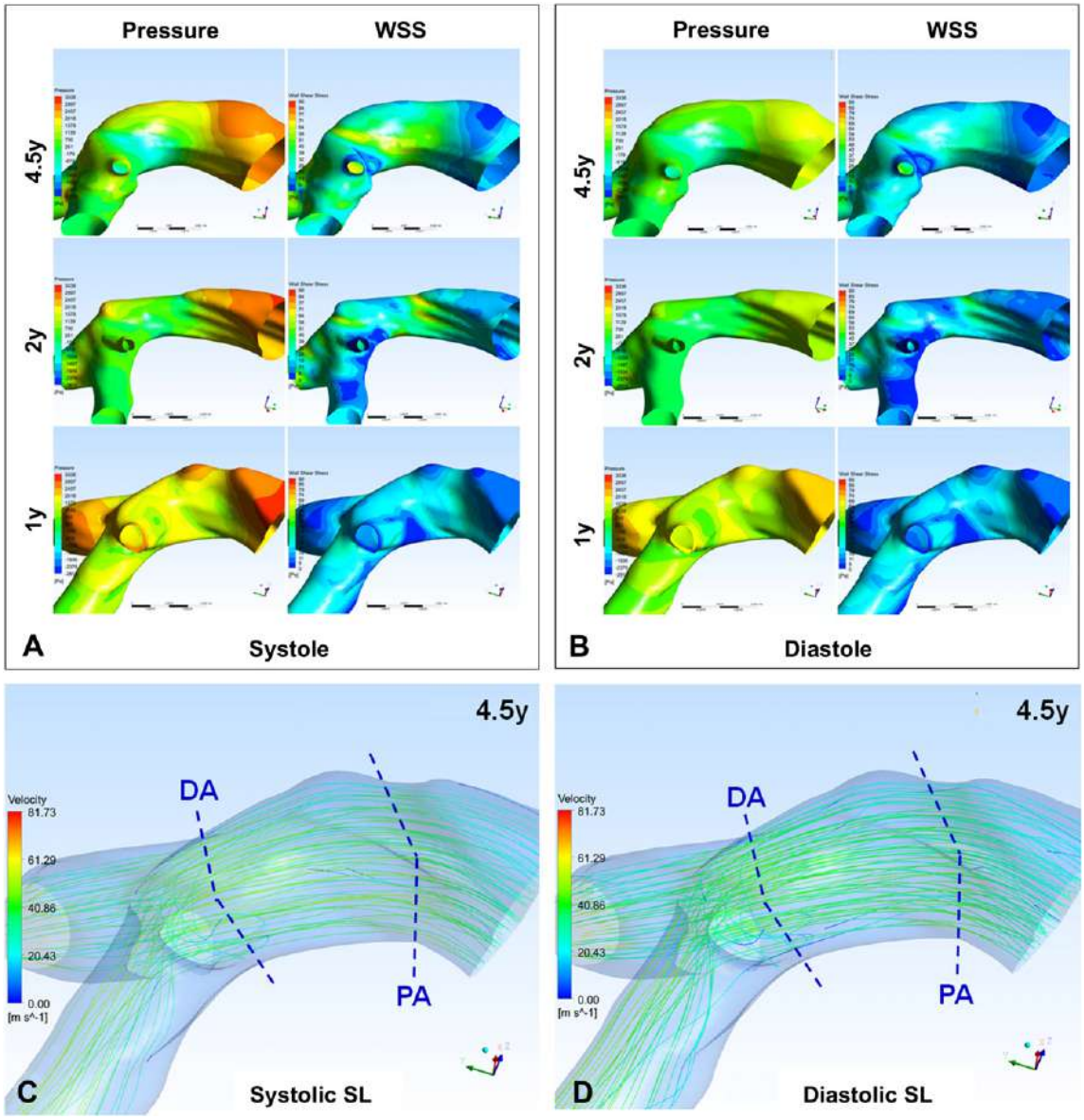

Fig. 5. Calculated wall pressure (Pa), wall shear stress (WSS) (Pa) and velocity-coded streamlines (m/s) in the pulmonary trunk during systoly and diastoly of three different sheep, 50, 100 and 240 weeks after implantation of the tissue engineered graft. The flow pattern remains to be smooth with low wall shear stress during the systoly especially after 240 weeks, although the pressure is slightly higher. The low shear stress and the absence of turbulences indicate that no significant wall irregularities, as e.g. atherosclerosis, aneurysms or scars, are present. The location of the TEVG in the 3D-CT-streamline-reconstructions is indicated using parantheses (see blue lines in the corrected figure version; PA = proximal anastomosis; DA = Distal anastomosis) (For interpretation of the references to colour in this figure legend, the reader is referred to the web version of this article.).

4. Discussion

Tissue engineering technologies aiming at the *in vitro* fabrication of cell based, living tissue and organ replacements have created substantial clinical hope and expectations. Particularly for pediatric applications, the growth potential of tissue engineered grafts addresses an unmet medical need since currently available artificial prostheses inherently lack growth capacity. In initial, long-term preclinical large animal trials, we and others have demonstrated functionality and growth of living tissue engineered autologous vascular grafts [3,25–28]. Tissue engineered vascular grafts were successfully applied to the low [27] as well as to the systemic pressure system [28] in animal models and the translation into a clinical setting using human cells has also been demonstrated [29,30]. The group of Shin'oka and colleagues [31,32] were the first entering the clinical arena and recently reported initial clinical results on vascular autografts generated from human bone marrow cells [32].

However, so far the impact of the biological cell age and resulting tissue functionality associated with the extensive, multiple-step tissue engineering process is not understood and has not been evaluated. Accelerated cell aging and senescence due to the extensive *in vitro* manipulations inherent to tissue engineering technologies may lead to complications and tissue dysfunction [10,11,17,19]. Therefore, a meticulous understanding of such effects and the implementation of quality markers represent a prerequisite for safe routine translation of tissue engineering technologies into clinical practice [3].

Here, using telomere length analysis technologies, significant differences in the biological age between tissue engineered and native vessels up to 100 weeks post-transplantation were observed whereas these differences were absent after 240 weeks. In parallel,

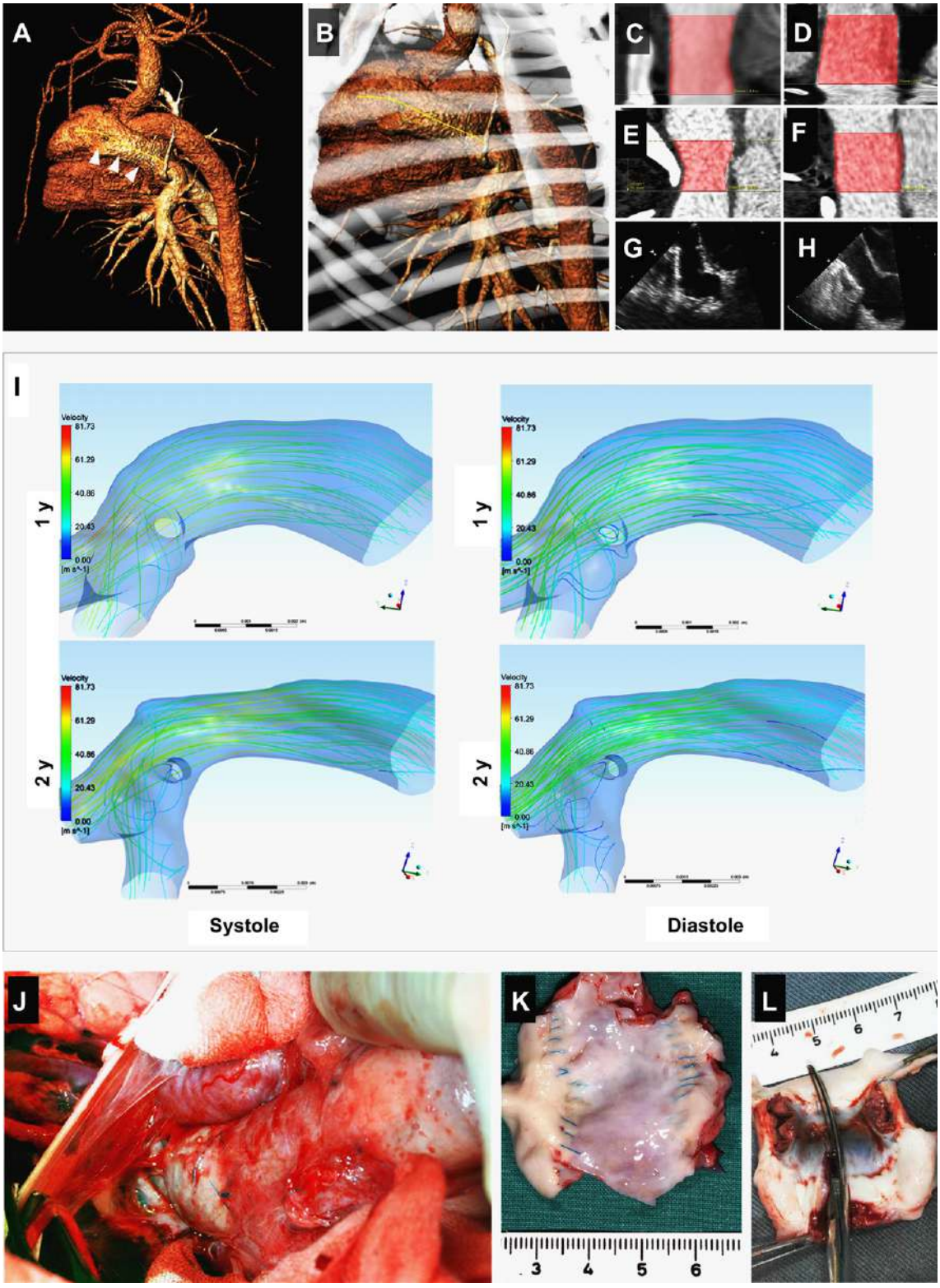

Fig. 6. 3D-reconstruction based on CT dataset with and without the rips showing the cardiovascular structure of the ovine chest. The yellow line depicts the pulmonary artery replacement (A and B). The volumetry of 2 cm length of the pulmonary artery replacement showed a volume increase from 6.4cc (C, 20 weeks), (D, 50 weeks), (E, 100 weeks) to 13,2cc (F, 240 weeks). Exemplary, trans-oesophageal echocardiography at 50 weeks (G) and 240 weeks (H) displayed no signs of malfunction or degeneration such as thrombus formation, calcification, stenosis, suture dehiscence, or aneurysm formation. Corresponding to the flow simulation after 240 weeks (Fig. 3C and D), the CT reconstruction displayed a similar smooth flow pattern after 1 and 2 years without any signs of stenosis, aneurysm or thrombus formation (I). This was in line with the macroscopic findings 240 weeks after implantation (J–K). Before harvest, the TEVG appeared to be fully integrated into the surrounding tissue without any signs of aneurysm or dehiscence (J) and after harvest, the initial suture lines could be easily identified confirming that there were no signs of degeneration or thrombotic events (For interpretation of the references to colour in this figure legend, the reader is referred to the web version of this article.).

histological results revealed clear border zones between the TEVG and the native vessel after 20 weeks post implantation. These distinct border zones became less prominent after 100 weeks and indistinguishable after 240 weeks, suggesting the completion of tissue remodeling processes beyond the period of 100 weeks. These observations, together with results demonstrating an increased DNA content and mechanical maturation over time in the TEVGs [3], lead to three different assumptions regarding the fate of the cells within the TEVGs:

(i) despite intensive *in vitro* expansion the cells used to colonize the vascular graft remain proliferative *in vivo* and further maturate to a functional vessel replacement. The alignment in telomere length after 240 weeks is solely due to biological aging of the native PA. This hypothesis is supported by the observation that we couldn't detect changes in the relative telomere ratio TEVG to native PA even at the 100 weeks' time point. One would have expected that the repopulating cells leveling the overall telomere length ratio of TEVG and native PA after 100 weeks according to the DNA quantification in Hoerstrup et al 2006 (3) (ii) the cells are replaced by native cell populations which are subjected to an accelerated biological aging due to a higher frequency of cell division required to re-populate the vascular graft. This would lead to an alignment of both populations over time as seen after 240 weeks. This mechanism is supported by the histological analysis demonstrating an ingrowth of native cell populations from the sides of anastomosis. (iii) Most likely, both mechanisms are coming into place during the remodeling process of the TEVG depending on the spatial localization within the graft. Cell ingrowth from the sides of anastomosis remodel the border zones as well as proliferation and maturation of the inherent TEVG cell populations (Fig. 7). Apart from this intrinsic as well as trans-anastomotic cellularization of the TEVGs, also blood-borne cellular repopulation may play a significant role in the process of TEVG repopulation. For the future clinical application of TEVGs, tissue remodeling mechanisms have to be evaluated in more detail to better control the safety of tissue engineered transplants. Even though the biological age of the TEVGs was higher than the native PA, our results show that these phenomena did not affect the functionality of the TEVGs. Using novel CT imaging analysis tools such as 3D reconstruction flow simulations and 3D vessel volumetric measurements, full functionality and growth of the TEVGs for up to 240 weeks was demonstrated. The flow simulation analysis revealed physiological parameters including stable wall pressures, low shear stresses and velocity patterns in the TEVGs over the whole follow up period. In particular, the low wall shear stress and the absence of turbulences displayed native analogous vascular performance and absence of aneurysm formation or dilatation. When taking the results of the 3D vessel volumetric into account, continuous functional growth was confirmed which was in line with the general body weight increase of the animals. These findings are in line with the recent study of Brennan et al who performed intrathoracic inferior caval vein replacements using bone marrow mononuclear cell derived TEVGs in a juvenile lamb model [25]. The authors serially performed a 3D magnetic resonance imaging (MRI) volume analysis over the period of six months and demonstrated continuous size increase of the TEVGs suggesting functional growth [25].

By integrating cell biology and functional analyses it is demonstrated that TEVGs replacing pulmonary arteries exhibit higher biological age but maintain full functionality in the absence of signs of dysfunctional degeneration, such as calcification, stenosis, thromboembolic events or aneurysm formation. To our knowledge, this is the first time that results demonstrating the performance of living, autologous tissue engineered grafts over almost 5 years in a full growth animal model are available. As it has been reported that follow-up periods in a lamb model can be extrapolated to a four- to fivefold period of time in humans [33], these results may be considered as important safety information before entering first-in-man clinical trials. In the light of the fact that sheep represent a `worst case model' due to the elevated calcium metabolism allowing for the evaluation of degenerative processes of cardiovascular implants [3], our results indicate long-term safety also with regard to calcific tissue degeneration beyond the growth phase of TEVGs.

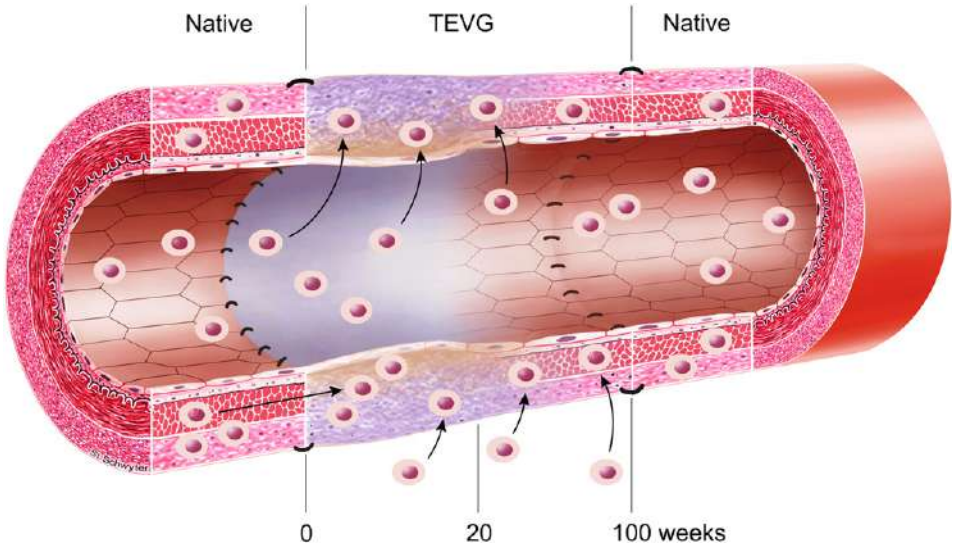

Fig. 7. Schematic diagram depicting the mechanism of TEVG remodeling and functional healing response: The disappearance of cells with shortened telomere lengths over time demonstrates the endogenous replacement of the originally seeded cells. After implantation of the TEVG a function healing response occurs (0–20 weeks), which is accompanied by a transient inflammatory response, cellular in-growth and repopulation of endogenous cells into the TEVG. A pannus containing a-SMA and desmin cells has formed at the luminal surface (neointima) and granulation tissue evolving into fibrous tissue containing glycosaminoglycans and collagen. These cells originate from different sources and approach the TEVG via different mechanisms including the trans-anastomotic in-growth (i), blood derived cell immigration (ii), or adventitia derived cell migration (iii). Whereas the interface between the TEVG and the native PA is still detectable within the period of 20–100 weeks it is equalized after a 100 weeks and fully integrated and indistinguishable after 240 weeks *in vivo* indicating completion of tissue remodeling beyond 100 weeks.

5. Conclusions

Extensive *in vivo* remodeling processes and endogenous cellular replacement appear to be the basis for the observed functionality. Based on these findings functional tissue engineering could be characterized as a "guided functional healing" process based on living, autologous cellular starter constructs. We demonstrate that TEVGs exhibit an increased biological age while maintaining full functionality. Using novel CT imaging analysis tools, the absence of dysfunctional degeneration, such as calcification, stenosis, thromboembolic events, and graft dilatation or aneurysm formation was confirmed. As these results can be extrapolated to an age of approx. 20 years in humans this study adds further information as to the clinical safety of autologous tissue engineering technologies.

Disclosures

S.P.H. and G.Z. are scientific advisors of Xeltis AG, Switzerland.

Acknowledgments

We thank Rene Stenger, BSc for his scientific and technical support. We thank B. Leskoschek and the entire team of the Department of Surgical Research for their support. Dr. Emmert was supported by the SPUM (Special Program University Medicine; Swiss National Science Foundation).

Appendix A. Supplementary materials

Supplementary data related to this article can be found online at http://dx.doi.org/10.1016/j.biomaterials.2012.07.049.

References

[1] Marelli AJ, Mackie AS, Ionescu-Ittu R, Rahme E, Pilote L. Congenital heart disease in the general population: changing prevalence and age distribution. Circulation 2007;115:163–72.
[2] Alexi-Meskishvili V, Ovroutski S, Ewert P, Dahnert I, Berger F, Lange PE, et al. Optimal conduit size for extracardiac Fontan operation. Eur J Cardiothorac Surg 2000;18:690–5.
[3] Hoerstrup SP, Cummings I, Lachat M, Schoen FJ, Jenni R, Leschka S, et al. Functional growth in tissue-engineered living, vascular grafts: follow-up at 100 weeks in a large animal model. Circulation 2006;114:159–66.
[4] Mol A, Smits AI, Bouten CV, Baaijens FP. Tissue engineering of heart valves: advances and current challenges. Expert Rev Med Devices 2009;6:259–75.
[5] Schmidt D, Dijkman PE, Driessen-Mol A, Stenger R, Mariani C, Puolakka A, et al. Minimally-invasive implantation of living tissue engineered heart valves: a comprehensive approach from autologous vascular cells to stem cells. J Am Coll Cardiol 56:510–520.
[6] Sodian R, Lemke T, Fritsche C, Hoerstrup SP, Fu P, Potapov EV, et al. Tissue-engineering bioreactors: a new combined cell-seeding and perfusion system for vascular tissue engineering. Tissue Eng 2002;8:863–70.
[7] Isenberg BC, Williams C, Tranquillo RT. Small-diameter artificial arteries engineered in vitro. Circ Res 2006;98:25–35.
[8] L'Heureux N, Dusserre N, Marini A, Garrido S, de la Fuente L, McAllister T. Technology insight: the evolution of tissue-engineered vascular grafts–from research to clinical practice. Nat Clin Pract Cardiovasc Med 2007;4:389–95.
[9] Allsopp RC, Chang E, Kashefi-Aazam M, Rogaev EI, Piatyszek MA, Shay JW, et al. Telomere shortening is associated with cell division in vitro and in vivo. Exp Cell Res 1995;220:194–200.
[10] Chang E, Harley CB. Telomere length and replicative aging in human vascular tissues. Proc Natl Acad Sci USA 1995;92:11190–4.
[11] Hao LY, Armanios M, Strong MA, Karim B, Feldser DM, Huso D, et al. Short telomeres, even in the presence of telomerase, limit tissue renewal capacity. Cell 2005;123:1121–31.
[12] Demerath EW, Cameron N, Gillman MW, Towne B, Siervogel RM. Telomeres and telomerase in the fetal origins of cardiovascular disease: a review. Hum Biol 2004;76:127–46.
[13] Bekaert S, De Meyer T, Rietzschel ER, De Buyzere ML, De Bacquer D, Langlois M, et al. Telomere length and cardiovascular risk factors in a middle-aged population free of overt cardiovascular disease. Aging Cell 2007;6:639–47.
[14] Chiang YJ, Calado RT, Hathcock KS, Lansdorp PM, Young NS, Hodes RJ. Telomere length is inherited with resetting of the telomere set-point. Proc Natl Acad Sci U S A 107:10148–53.
[15] Fuster JJ, Andres V. Telomere biology and cardiovascular disease. Circ Res 2006;99:1167–80.
[16] De Meyer T, Rietzschel ER, De Buyzere ML, Langlois MR, De Bacquer D, Segers P, et al. Systemic telomere length and preclinical atherosclerosis: the Asklepios study. Eur Heart J 2009;30:3074–81.
[17] De Meyer T, Rietzschel ER, De Buyzere ML, Van Criekinge W, Bekaert S. Telomere length and cardiovascular aging: the means to the ends? Ageing Res Rev 2011;10:297–303.
[18] Saliques S, Zeller M, Lorin J, Lorgis L, Teyssier JR, Cottin Y, et al. Telomere length and cardiovascular disease. Arch Cardiovasc Dis 103:454–459.
[19] Edo MD, Andres V. Aging, telomeres, and atherosclerosis. Cardiovasc Res 2005;66:213–21.
[20] Poon SS, Lansdorp PM. Quantitative fluorescence in situ hybridization (Q-FISH). Curr Protoc Cell Biol 2001 [Chapter 18]:Unit 18 14.
[21] Delibasis KS, Matsopoulos GK, Mouravliansky NA, Nikita KS. A novel and efficient implementation of the marching cubes algorithm. Comput Med Imaging Graph 2001;25:343–52.
[22] Rajon DA, Bolch WE. Marching cube algorithm: review and trilinear interpolation adaptation for image-based dosimetric models. Comput Med Imaging Graph 2003;27:411–35.
[23] Frauenfelder T, Lotfey M, Boehm T, Wildermuth S. Computational fluid dynamics: hemodynamic changes in abdominal aortic aneurysm after stent-graft implantation. Cardiovasc Intervent Radiol 2006;29:613–23.
[24] Das B, Saini D, Seshadri M. Telomere length in human adults and high level natural background radiation. PLoS One 2009;4:e8440.
[25] Brennan MP, Dardik A, Hibino N, Roh JD, Nelson GN, Papademitris X, et al. Tissue-engineered vascular grafts demonstrate evidence of growth and development when implanted in a juvenile animal model. Ann Surg 2008;248:370–7.
[26] Dahl SL, Kypson AP, Lawson JH, Blum JL, Strader JT, Li Y, et al. Readily available tissue-engineered vascular grafts. Sci Transl Med 2011;3:68ra69.
[27] Shinoka T, Shum-Tim D, Ma PX, Tanel RE, Isogai N, Langer R, et al. Creation of viable pulmonary artery autografts through tissue engineering. J Thorac Cardiovasc Surg 1998;115:536–45.
[28] Shum-Tim D, Stock U, Hrkach J, Shinoka T, Lien J, Moses MA, et al. Tissue engineering of autologous aorta using a new biodegradable polymer. Ann Thorac Surg 1999;68:2298–305.
[29] Hoerstrup SP, Kadner A, Melnitchouk S, Trojan A, Eid K, Tracy J, et al. Tissue engineering of functional trileaflet heart valves from human marrow stromal cells. Circulation 2002;106:143–50.
[30] Poh M, Boyer M, Solan A, Dahl SL, Pedrotty D, Banik SS, et al. Blood vessels engineered from human cells. Lancet 2005;365:2122–4.
[31] Shin'oka T, Imai Y, Ikada Y. Transplantation of a tissue-engineered pulmonary artery. N Engl J Med 2001;344:532–3.
[32] Shin'oka T, Matsumura G, Hibino N, Naito Y, Watanabe M, Konuma T, et al. Midterm clinical result of tissue-engineered vascular autografts seeded with autologous bone marrow cells. J Thorac Cardiovasc Surg 2005;129:1330–8.
[33] Barnhart GR, Jones M, Ishihara T, Rose DM, Chavez AM, Ferrans VJ. Degeneration and calcification of bioprosthetic cardiac valves. Bioprosthetic tricuspid valve implantation in sheep. Am J Pathol 1982;106:136–9.